

Systematic Surface Scan of the Most Favorable Interaction Sites of Magnesium Ions with Tetracycline

Olaf G. Othersen, Harald Lanig, and Timothy Clark*

Computer-Chemie-Centrum, Universität Erlangen-Nürnberg,
Nägelsbachstrasse 25, 91052 Erlangen, Germany

Received September 22, 2003

Abstract: AM1 semiempirical molecular orbital calculations have been used to probe the complexation sites for naked and hydrated magnesium ions to the different conformations and protonation states of tetracycline. The calculations reveal a wealth of possible magnesium complexation sites within a small energy range, but also indicate that magnesium complexation does not change the conformational behavior of tetracycline significantly. A hitherto unknown solvated conformation is suggested for deprotonated tetracycline.

Introduction. Tetracycline (Tc) and its analogues have gained considerable importance, not only as broad spectrum antibiotics,¹ since their discovery in 1947.² More recently, tetracyclines have become more significant through their use as regulators of biological function because of their interaction with tetracycline repressor regulatory proteins (TetR).³ However, the physical chemistry of the tetracyclines is still poorly understood, despite their clinical importance and their extremely widespread use in microbiology. Schneider⁴ has described the tetracyclines as “chameleon-like” because of their ability to adopt different conformations, protonation states, and tautomers, depending on the conditions. We recently reported an extended density functional theory (DFT) study⁵ of the conformations and tautomers of neutral Tc in aqueous solution. The starting conformations for this study were obtained by a very extensive conformational search⁶ using molecular dynamics and AM1 semiempirical molecular orbital theory. However, factors such as metal complexation may affect the structure of Tc significantly,⁴ so that conclusions based on neutral solution do not necessarily apply to those containing metal ions. Of special importance in this respect is Mg^{2+} . The ligand for the induction of TetR is actually a Tc: Mg^{2+} complex,⁷ but the complexation behavior of Tc with Mg^{2+} is by no means clear.^{4,8} We therefore now report an AM1 study of the possible complexation sites for a single magnesium ion (both alone and solvated with four or five waters) on the surface of Tc. We include the most common tautomers of neutral Tc and its monodeprotonated anion.

Computational Methods. All semiempirical calculations were performed using the program VAMP 7.5a⁹ with the AM1¹⁰ Hamiltonian. Magnesium parameters were taken from Hutter et al.¹¹ The COSMO¹² continuum solvent model was used to simulate a water solution. Calculation of root-mean-square deviations (RMSD) were performed with QUATFIT¹³ and the statistical analyses with TSAR 3.3.¹⁴

Structure Generation. Published gas-phase structures of Tc in different protonation patterns and conformations⁶ served as the geometrical basis for all

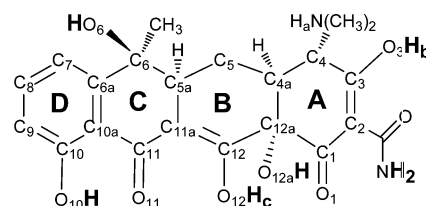


Figure 1. Structure template of the protonation states of tetracycline, distinguished by the hydrogens H_a, H_b, or H_c.

subsequent calculations. Figure 1 shows Tc in the different protonation states investigated: hydrogen atoms H_b and H_c are present in the neutral form (N), H_a and H_c in the zwitterionic form (Z), and H_a in the zwitteranionic form (A). For each of these structures, hydrogen atoms bonded to oxygen or the amide group (Figure 1, larger, bold hydrogen atoms) were removed prior to the calculation of a modified solvent-accessible surface (SAS). A magnesium-ion radius of 0.66 Å¹⁵ was used as probe radius for the surface generation. The resolution for the triangulation was adjusted to generate approximately 1400 surface points. For each point, a Tc: Mg^{2+} structure was generated by substituting this surface point with a magnesium ion and restoring the previously deleted hydrogen atoms, rotated to avoid bad van der Waals contacts. The restored hydrogen atoms were optimized, and the heat of formation was calculated. Subsequent analyses were performed for all local minima on the nine energy hypersurfaces (three different conformations for each of the three protonation states) thus obtained that lie within 15 kcal mol⁻¹ of the absolute minimum.

For the metal-ion binding sites identified, water-complexation spheres for magnesium with both four and five water molecules were generated as described in the Supporting Information. The resulting Tc: Mg^{2+} -complexes with zero, four and five water molecules were then optimized in a stepwise procedure in order to minimize the influence of the starting positions of the water molecules. In the first step the magnesium position was fixed and Tc was kept rigid, in the second step only Tc was kept rigid and finally the complete structure was optimized.

Structure Analysis. The resulting 495 geometries were clustered by their carbon-atom scaffold (only the carbon atoms of the polycyclic ring system, Figure 1, C₁ to C_{12a}) dihedral angles, ignoring angles with a range of less than 20° and strongly correlated ones (correlation coefficient ≥ 0.95). The distance of the magnesium positions and the RMSD for the complete scaffold compared to the X-ray structure of Tc in the induced TetR (PDB-entry: 2trt¹⁶) were also calculated. Hydrogen interactions were counted if a hydrogen bonded to oxygen or nitrogen was less than 2.5 Å away from another electronegative atom.

The Boltzmann population was calculated for every structure using the minimum energy for each protonation pattern and total formula as reference. To compare the heats of formation calculated for the solvated structures with the energy of the Tc present in the protein environment, the inducer–Mg complex was extracted from the X-ray structure, and hydrogen atoms

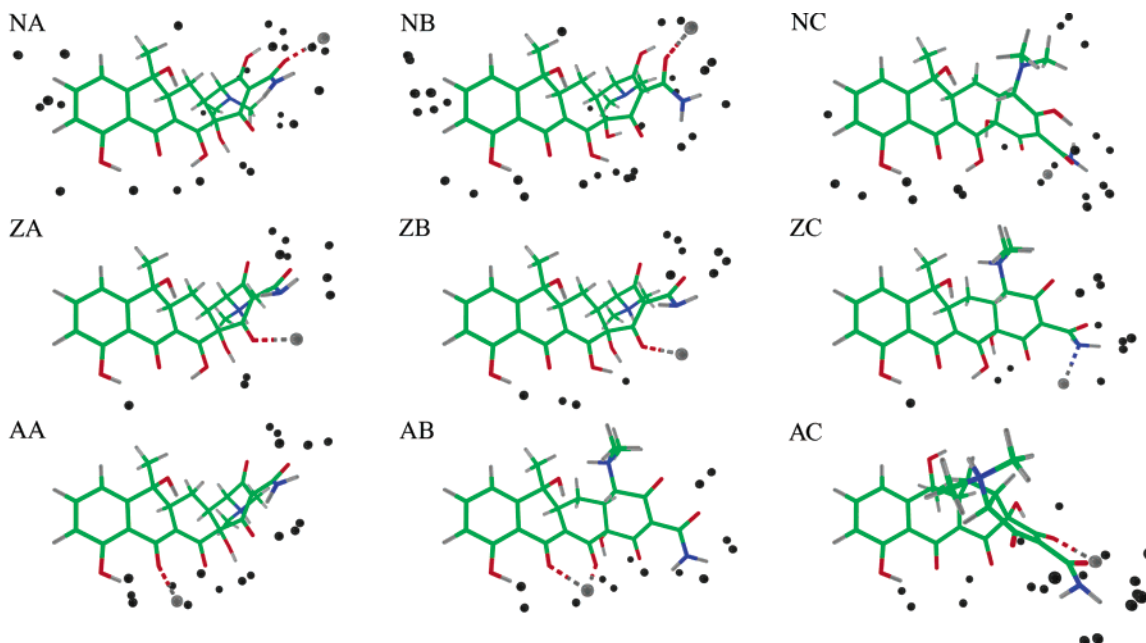


Figure 2. Calculated interaction sites of magnesium ions with tetracycline in different protonation patterns and conformations. The gray sphere shows the energetically most favorable magnesium position. Dashed bonds mark a distance less than 110% of the sum of the van der Waals radii involved. Black spheres show local minima that differ in energy less than 15 kcal mol⁻¹ from the absolute minimum. Top to bottom: protonation patterns (N, Z, and A). Left to right: scaffold conformations (A, B, and C).

and water molecules were added to obtain the protonation patterns investigated with zero, four, and five water molecules. The geometries were optimized using weak harmonic restraints (20.0 kcal mol⁻¹ Å⁻²) on the positions of the tetracycline heavy atoms.

Results. For all protonation states, the geometry optimization using the COSMO solvent model generally resulted in the relaxation of the most twisted gas-phase structures to a more extended conformation. We have noted previously⁵ that the extended conformation¹⁷ is stabilized preferentially by solvation. For the neutral and the zwitterionic forms, two of the three initial conformations relaxed to very similar local minima, as found in our DFT study.⁵ The zwitteranionic conformations also extend, but to different scaffold geometries.

Metal-ion interaction sites (Figure 2) for the rigid scaffolds are located near the amide group and along the chain of oxygen atoms O₁, O_{12a}, O₁₂, O₁₁, and O₁₀ (Figure 1), sparsely populated in the case of the zwitterionic form. Neutral conformations show additional interaction sites at the aromatic ring D, next to the methyl groups of the amine and adjacent to the oxygen and the methyl group attached to C₆ (only NA and NB, see Figure 2). The most stable interaction site for a magnesium ion is localized at the amide group with the exception of two zwitteranionic conformations (AA and AB), where magnesium interacts with the oxygens O₁₁ and O₁₂.

The cluster analysis of the optimized geometries resulted in four different groups (Figure 3). Cluster 1 is very similar to the X-ray structure of Tc bound to the induced TetR (RMSD (cluster center-X-ray) = 0.378 Å). This cluster represents the main population for all protonation patterns (N, Z, and A) and also contains the absolute minima of each protonation pattern/water complexation state. Cluster 2 differs from the X-ray geometry in the conformation of ring A and contains almost only neutral conformations. In cluster 3, which

contains almost exclusively zwitterionic and zwitteranionic protonation patterns, this deviation expands to ring B. The final cluster, 4, shows another folded conformation populated only by energetically unfavorable zwitteranionic molecules.

The absolute minima for the different protonation patterns and water-complexation spheres are located between O₁₂ and O₁ for all zwitteranionic structures and the neutral structures with explicit water. The zwitterionic minima and the minima for the neutral form without water are located between the nitrogen of the amide group and O₁. Additional energetically favored interaction sites in each cluster are located at the amide group and at the oxygens O₁₀, O₁₁, O₁₂, and O_{12a}. In clusters 2 and 3, a further interaction site was found between the nitrogen of the dimethylamino group and O₆.

Cluster-dependent analysis of the hydrogen-bond network shows that a hydrogen bond between the protonated nitrogen of the amine as donor and O_{12a} directs the structure into cluster 1. If the acceptor of this bond is O₆, the structure is assigned to clusters 2 or 3, which correspond to the twisted conformation discussed in the literature.¹⁷ Another structure-influencing hydrogen bond donor is O_{12a}. If the acceptor is the amine nitrogen or O₁₂, the structure is assigned to cluster 1. Structures with O₁₂H...O₁ and O₁₂H...O_{12a} interactions are found mainly in cluster 1 (with one exception each in clusters 2 and 3 for the O₁₂H...O₁ hydrogen bond), while O₁₂H...O₁₁ and O_{12a}H...O₁ hydrogen bonds are found in each cluster.

The influence of the explicit water-complexation sphere on the scaffold conformation is small. 97% of the Tc:Mg²⁺ starting structures, although containing a different number of water molecules, fall into the same cluster as found without explicit water. On the other hand, 30% of the structures differ by more than 2 Å in

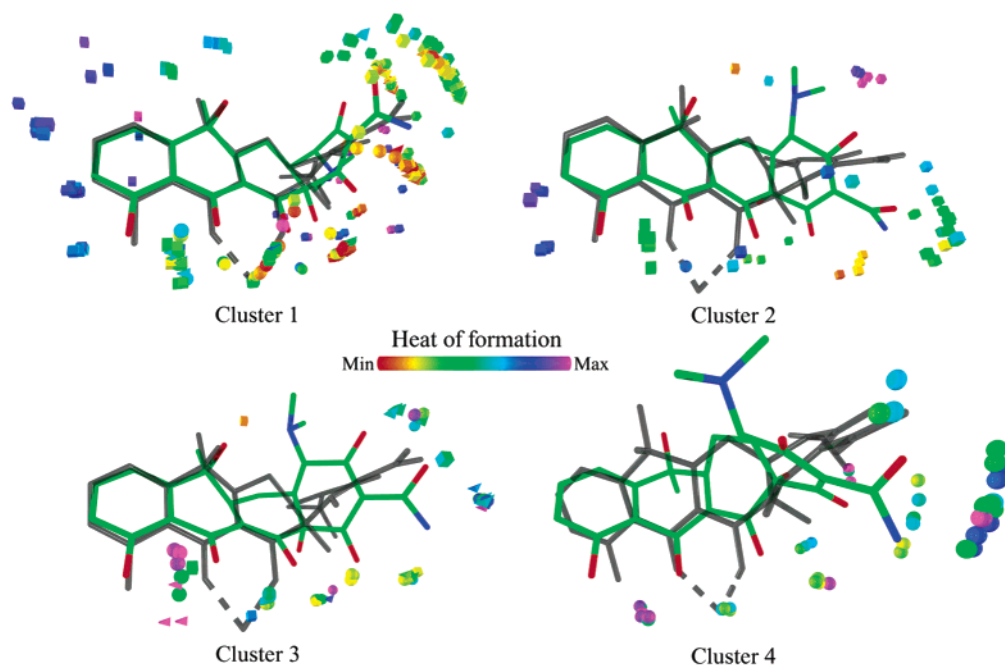


Figure 3. Cluster centers and magnesium ion positions, superimposed on X-ray structure of Tc:Mg²⁺, present in the induced TetR (translucent gray, dashed bonds point to the X-ray position of magnesium). The calculated magnesium positions, shown as boxes (neutral form N), tetrahedrons (zwitterionic form Z), and spheres (zwitteranionic form A), are colored by their heat of formation. For clarity, all hydrogen atoms are omitted.

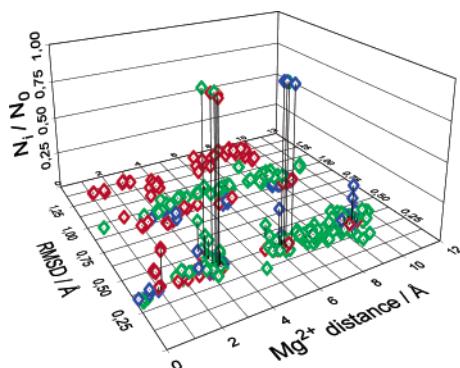


Figure 4. Boltzmann population depending on the RMSD and the Mg²⁺ distances to the X-ray geometry. Neutral forms (N) are colored green, zwitterionic forms (Z) blue, and zwitteranionic forms (A) red. The dropdown lines clarifies the corresponding base plane positions.

the positions of the magnesium ions, demonstrating the influence of solvation on the magnesium-complexation site.

Boltzmann populations were calculated for every structure of each protonation pattern and water coordination. Figure 4 shows the resulting populations plotted on a grid whose axes are the distance between the magnesium positions and the RMSD of the actual scaffold structure, both compared to the X-ray geometry. Areas with a high Boltzmann population are located at an RMSD of 0.4 Å and magnesium distances of about 1, 3, 6, and 9 Å. Note that there is a zwitteranionic structure with an energy only 0.96 kcal mol⁻¹ above the corresponding absolute minimum with a low RMSD to the X-ray geometry and a small distance in the magnesium position (Figure 5).

The restrained optimized tetracyclines show a heavy atom RMSD between the different protonation patterns and the X-ray geometry of about 0.08 Å. The differences

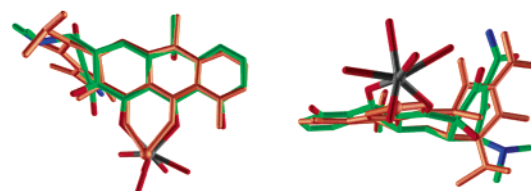


Figure 5. Rear and side view of an energetic favored zwitteranionic conformation (CPK-colored) with low RMSD to the X-ray geometry (orange). All hydrogen atoms are omitted for clarity.

Table 1. Energy Differences (kcal mol⁻¹) between the Absolute Minimum and the X-ray Geometry Optimized with Restraints

protonation pattern	0 water	4 water	5 water
neutral	20.7	22.5	21.6
zwitterionic	25.6	25.5	25.6
zwitteranionic	15.2	19.2	13.9

in the heat of formation between the X-ray geometries and the absolute minima are shown in Table 1.

Discussion. Our calculations show that the extended conformation of the Tc:Mg²⁺ complexes is energetically favored over the twisted conformation¹⁷ (cluster 2 and 3) by about 2.2 and 3.6 kcal mol⁻¹, respectively. This is in accordance with the DFT results obtained for neutral, metal-free Tc,⁵ suggesting that metal complexation does not influence the conformational behavior of Tc significantly. The twisted conformation divides into two because the protonation of the dimethylamino group increases steric demand and pushes C₅ away. Therefore, nearly all zwitterionic and zwitteranionic twisted conformations are accumulated in cluster 3 and the neutral structures in cluster 2. Cluster 4, which has not been described explicitly in solvent to date, contains unique zwitteranionic conformations about 5.8 kcal mol⁻¹ less stable than the reference. Similar conformations have been reported for all protonation patterns in the gas

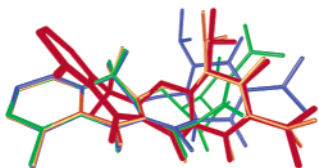


Figure 6. Superimposition of the obtained cluster centers. Cluster 2 (orange) and 3 (blue) are superimposed by ring C and D with cluster 1 (green), cluster 4 (red) by ring A and B on cluster 2. All hydrogen atoms are omitted for clarity.

phase,⁶ but in solvent only the zwitteranionic structures represent local minima. Cluster 4 exhibits the twisted conformation and resembles cluster 2, but contains a flip of the C₆ atom. The value of the C₇–C_{6a}–C₆–C_{5a} dihedral angle is about 145°, compared to –145° in the other clusters (Figure 6). The cluster is not specially stabilized by a defined hydrogen-bond network or preferred magnesium positions, but shows the same metal-interaction sites as the other clusters. Although the Boltzmann population of this conformation is very small, the unusual behavior and properties of Tc suggest that it should not be neglected.

The magnesium-interaction sites are spread over wide regions on the Tc surface with only minor differences in energy. This could explain the different chelation sites for the metal ion in the literature.^{8,18}

Our results allow us to identify most of the hydrogen bonds required for the generation of the extended and twisted conformations.^{5,8} An exception is the O_{12a}H···O₁ hydrogen bond, which was found to be specific for the twisted conformation in DFT calculations,⁵ but is rather unspecific in the present AM1 calculations. The calculations also suggest that O₁₂H···O₁ and O₁₂H···O_{12a} hydrogen interactions direct the structure toward the extended conformation. The presence of a hydrogen bond is sufficient to classify the structure into a distinct conformation, whereas its absence contains no cluster information. One reason is that a magnesium ion easily inserts into the hydrogen-bond network, leading to structural rearrangements.

The calculated energies in solution suggest significantly populated conformations that are very similar to the geometry of Tc in the induced TetR crystal structure. Tc must therefore undergo only minor changes in solution upon binding to the repressor protein. On the other hand, the magnesium positions in solution do not match well with the X-ray geometry. This is, however, probably not energetically significant because the magnesium position can be changed at little cost in energy. However, a stable zwitteranionic structure very similar to the X-ray geometry exists in solution (Figure 5).

Comparing absolute minima of the heat of formation resulting from the scan process with the energy of the matching, restrained optimized X-ray geometry (Table 1), shows that about 7 kcal mol⁻¹ less energy is needed to distort the zwitteranion to the bound structure than for either of the neutral species.

Conclusion. The systematic surface scan procedure presented here serves to identify metal-ion interaction sites for molecules with different possible protonation

patterns and conformations, with special emphasis on the hydrogen bond network. It leads to an increased understanding of the geometrical and energetic properties of tetracycline and serves as a starting point for more accurate but less comprehensive DFT studies.

Acknowledgment. We thank the Deutsche Forschungsgemeinschaft for financial support as part of Sonderforschungsbereich 473 (Mechanisms of Transcriptional Regulation) and the Graduiertenkolleg 805/1-02 (Protein-Protein interactions). H.L. thanks the Fonds der Chemischen Industrie for financial support.

Supporting Information Available: Protocol used to calculate the water sphere geometries. Calculated geometries and energies for the most stable representatives of each species in each of the clusters. This material is available free of charge via the Internet at <http://pubs.acs.org>.

References

- (1) Putnam, L. E.; Hendricks, F. D.; Welch, H. Tetracycline, a new antibiotic. *Antibiot. Chemother.* **1953**, *3*, 1183–1186.
- (2) Nelson, M. L.; Park, B. H.; Levy, S. B. molecular Requirements for the Inhibition of the Tetracycline Antiport Protein and the Effect of Potent Inhibitors on the Growth of Tetracycline-Resistant Bacteria. *J. Med. Chem.* **1994**, *37*, 1355–1361.
- (3) Hillen, W.; Berens, C. Tetracyclin controlled gene regulation: from bacterial origin to eukaryotic tools. *BIOspektrum* **2002**, *8*, 355–358.
- (4) Schneider, S. Proton and metal ion binding of tetracyclines. *Tetracyclines in Biology, Chemistry and Medicine*; Birkhäuser Verlag: Basel, 2001; pp 65–104.
- (5) Othersen, O. G.; Lanig, H.; Clark, T. Conformations and Tautomers of Tetracycline. *J. Phys. Chem. B* **2003**, in press.
- (6) Lanig, H.; Gottschalk, M.; Schneider, S.; Clark, T. Conformational Analysis of Tetracycline using molecular Mechanical and Semiempirical MO–Calculations. *J. Mol. Model.* **1999**, *5*, 46–62.
- (7) Hinrichs, W.; Kisker, C.; Duevel, M.; Mueller, A.; Tovar, K.; Hillen, W.; Saenger, W. Structure of the Tet repressor-tetracycline complex and regulation of antibiotic resistance. *Science* **1994**, *264*, 418–420.
- (8) Wessels, J. M.; Ford, W. E.; Szymczak, W.; Schneider, S. The Complexation of Tetracycline and Anhydrotetracycline with Mg²⁺ and Ca²⁺: A Spectroscopic Study. *J. Phys. Chem. B* **1998**, *102*, 9323–9331.
- (9) Clark, T.; Alex, A.; Beck, B.; Chandrasekhar, J.; Gedeck, P.; Horn, A. H. C.; Hutter, M.; Martin, B.; Rauhut, G.; Sauer, W.; Schindler, T.; Steinke, T. VAMP 7.5a, Build 18: Erlangen 2.
- (10) Dewar, M. J. S.; Zebisch, E. G.; Healy, E. F.; Stewart, J. J. P. AM1: A New General Purpose Quantum Mechanical molecular Model. *J. Am. Chem. Soc.* **1985**, *107*, 3902–3909.
- (11) Hutter, M. C.; Reimers, J. R.; Hush, N. S. Modeling the Bacterial Photosynthetic Reaction Center. 1. Magnesium Parameters for Semiempirical AM1 Method Developed Using a Genetic Algorithm. *J. Phys. Chem. B* **1998**, *102*, 8080–8090.
- (12) Klamt, A.; Schuurmann, G. COSMO: a new approach to dielectric screening in solvents with explicit expressions for the screening energy and its gradient. *J. Chem. Soc., Perkin Trans. 2* **1993**, *5*, 799–805.
- (13) Heisterberg, D.; Labanowski, J. *Quatfit*; <http://www.ccl.net/ccal/software/SOURCES/C/quaternion-mol-fit>; Columbus, OH.
- (14) Grassy, G.; Blaney, F.; Bradshaw, J.; Huxley, P.; Lahana, R.; Snarey, M.; Tute, M. *TSAR 3.3*; Oxford.
- (15) Aylward, G. H.; Findlay, T. J. V. *Datensammlung Chemie in SI-Einheiten*; 2. ed.; VCH Verlagsgesellschaft: Weinheim, 1986; 12.
- (16) Protein Data Bank; <http://www.rcsb.org>.
- (17) Duarte, H. A.; Carvalho, S.; Paniago, E. B.; Simas, A. M. Importance of Tautomers in the Chemical Behavior of Tetracyclines. *J. Pharm. Sci.* **1999**, *88*, 111–120.
- (18) Lambs, L.; Decock-Le Révérend, B.; Kozłowski, H.; Berthon, G. Metal ion-tetracycline interactions in biological fluids. 9. Circular dichroism spectra of calcium and magnesium complexes with tetracycline, oxytetracycline, doxycycline, and chlortetracycline and discussion of their binding modes. *Inorg. Chem.* **1988**, *27*, 3001–3012.

JM034199C